GEOPHYSICAL RESEARCH LETTERS, VOL. 40, 1–5, doi:10.1002/grl.50632, 2013

Distinct manifestations of austral summer tropical intraseasonal oscillations

Fernando E. Hirata,[1] Peter J. Webster,[1] and Violeta E. Toma[1]

Received 6 May 2013; revised 4 June 2013; accepted 4 June 2013.

[1] Event-to-event intraseasonal convection is found to be significantly different from a canonical Madden-Julian oscillation (MJO). Nearly half of all austral summer events do not show the same initiation or propagation characteristics of canonical MJOs, although they meet some MJO criteria during their life cycles. Variations of intraseasonal convection fall within three distinct forms: the canonical MJO, an eastward decaying mode, and an eastward intensifying mode. This distinction offers important insights into the overall dynamics and predictability of tropical intraseasonal variability. Sea surface temperature anomalies generated during convective breaks are fundamental for canonical propagation and result from radiative forcing whose modulation is a consequence of large-scale wave dynamics. Eastward propagation seems to rely more on the state of the tropical atmosphere-ocean system before convective triggering than on the trigger itself. Eastward decaying events exhibit weaker wave-related anomalies. Alternatively, mechanisms driving intensification over Indonesia are very different from the first two categories.
Citation: Hirata, F. E., P. J. Webster, and V. E. Toma (2013), Distinct manifestations of austral summer tropical intraseasonal oscillations, *Geophys. Res. Lett.*, *40*, doi:10.1002/grl.50632.

1. Introduction

[2] Large-scale tropical intraseasonal (IS) convection over the Eastern Hemisphere warm pool presents striking event-to-event variations. The most prominent austral summer mode of variability within the IS frequency band in the region is the Madden-Julian oscillation (MJO). However, an important fraction of the total IS variance of tropical convection over the Indian and West Pacific Oceans does not necessarily exhibit the same features of the observed MJO archetypal that has been developed by the scientific community since it was first depicted by *Madden and Julian* [1971].

[3] Traditionally, the MJO is defined as a planetary-scale eastward propagation of convection with a period between 30 and 90 days, stronger over the tropical Indian Ocean and the West Pacific during austral summer [*Zhang*, 2005]. Although we do not challenge this notion, we hypothesize that it hinders the understanding and limits the potential predictability of a significant fraction of tropical IS variability. Around 40%–60% of the IS variance in tropical convection over the eastern Indian Ocean and the West Pacific fit the traditional MJO definition, as measured by the simultaneous amplitude of the principal components (PCs) associated with the first two empirical orthogonal functions (EOFs) of one or more atmospheric variables [*Wheeler and Hendon*, 2004]. This strategy reveals fundamental real-time information about the location and amplitude of the MJO around the tropics. Nevertheless, there is still a comparable percentage of IS variance that falls somewhere in between the coherent MJO signal and other large-scale disturbances that permeate the tropics. Some episodes of large-scale IS convection are similar to the MJO ideal during early stages of their life cycles but fail to propagate as far east as canonical events. Other events present much weaker or an absence of convective anomalies over most of the Indian Ocean but grow enough over the Maritime Continent (MC) to be often called MJOs. Such distinct manifestations of tropical IS convection are commonly excluded from the data set by studies focusing on the MJO, but some of them also produce strong convection and rainfall over the region, indicating a path to improve the prospects for overall IS predictability. Our main motivation for the present effort is to describe and explain significant differences within the broad spectrum of tropical IS variability that go beyond the classic MJO conception and seek a characterization of these differences.

[4] Our goal is to show that there are enough statistical and dynamical reasons to recognize the existence of more than one distinct form of large-scale tropical IS convective events, each being significantly different from the conventional MJO. In particular, we suggest that these differences should not be neglected nor treated simply as weak MJOs. To label them all as MJO events may diminish signal-to-noise ratio and lessen potential predictability. To neglect them completely may deprive us of a better understanding of IS convection growth and propagation and the different sectoral influences that these other categories possess, including unique teleconnection patterns. The premise of limited categories of IS events sheds light on outstanding issues about tropical dynamics on IS time scales and may represent an improvement in extended-range weather forecasts in regions where these signals are important.

2. Definition of Intraseasonal Events

[5] We adopt a statistical definition of tropical IS events that closely follows the arguments of *Kessler* [2001], which consistently identifies large-scale slow eastward propagating IS patterns over the warm pools. Band-passed (20–90 days) outgoing longwave radiation (OLR) data [*Liebmann and Smith*, 1996] averaged between 5°N and 5°S during the austral summer season (October–March, from 1979 to 2011) are decomposed to simple empirical orthogonal functions (EOFs) (Figure 1a). The first two EOF modes are significantly

Additional supporting information may be found in the online version of this article.

[1]School of Earth and Atmospheric Sciences, Georgia Institute of Technology, Atlanta, Georgia, USA.

Corresponding author: F. E. Hirata, School of Earth and Atmospheric Sciences, Georgia Institute of Technology, 311 Ferst Dr., Atlanta, GA 30332, USA. (fernando.hirata@eas.gatech.edu)

0094-8276/13/10.1002/grl.50632

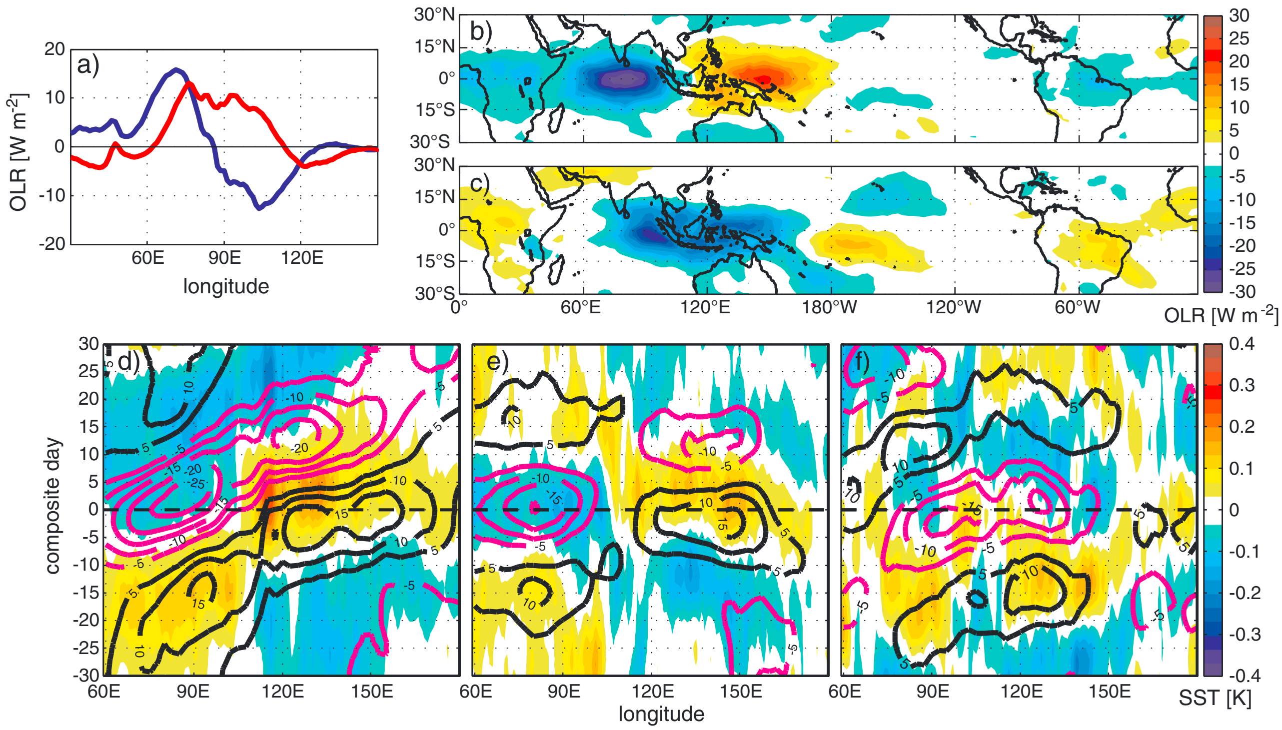

Figure 1. (a) Austral summer EOF modes of averaged (5°N–5°S) intraseasonal OLR. (b) Composite day 0 for PC1 events with a minimum below −1 standard deviation. (c) Composite day 0 for PC2 events with a minimum below −1 standard deviation. (d–f) Longitude-time diagrams of composite life cycles for MJO, ED, and EI events, respectively. Shading (contours) represents band-passed SST (OLR) anomalies averaged between 5°N and 10°S to highlight stronger SST anomalies south of the equator in the surroundings of the MC (Figure 2).

correlated with each other with maximum lag correlation of 0.65 when EOF1 principal component time series (PC1) leads EOF2 series (PC2) by approximately 11 days (Figure S1 in the supporting information). Together, they explain most of the IS variance over the Indian Ocean, the MC, and the West Pacific Ocean [*Kessler*, 2001]. Thus, these two modes are used to describe IS variations of large-scale convection and its following propagation over the tropics of the Eastern Hemisphere. Three sets of distinct large-scale IS convective events are defined as combinations of the patterns associated with EOF1 and EOF2 (Figures 1b and 1c).

[6] The first set encompasses the MJO: the fraction of planetary-scale IS convection that begins over the Indian Ocean initiation region and propagates eastward, reaching the western Pacific Ocean a few days later (Figure 1d). These events are defined when PC1 presents a minimum below −1 standard deviation and PC2 also falls below −1 standard deviation within 25 days after the PC1 minimum. The day of minimum PC1 value is the canonical MJO composite day 0. A second set of IS events is defined whenever PC1 presents a minimum below −1 standard deviation (this minimum is referred to as composite day 0 for this cycle), but a subsequent minimum below −1 standard deviation is not observed on PC2 within a period of 25 days. Events matching this criterion are referred to as *eastward decaying* (ED) events due to the observed weakening of convective activity over the MC (Figure 1e). The third category comprises IS events in which PC2 falls below −1 standard deviation (the composite day 0 for this cycle), but it is not preceded by a minimum on PC1 below −1 standard deviation. This last category describes weak or absent convection over the tropical eastern Indian Ocean that later strengthens over the MC (Figure 1f). These are referred to as *eastward intensifying* (EI) events. The threshold of 1 standard deviation is used to include relatively strong convective events and to state that ED and EI events are not necessarily the same as weak MJO events. An important result is that more than 40% of the total 93 IS events identified through this method do not fall into the MJO category (Table S1 in the supporting information) and agree well with estimates that the MJO accounts for nearly 60% of the IS variance [*Wheeler and Hendon*, 2004].

[7] Other variables used in this study were obtained from ERA-Interim Reanalysis data set. We also use NOAA's daily Optimum Interpolation (OI) AVHRR-only [*Reynolds et al.*, 2007] and Tropical Rainfall Measuring Mission Microwave Imager (TMI) 3 day average sea surface temperature (SST) data [*Wentz*, 1997]. All data were band passed using the same procedure applied to OLR. Gaps in TMI data were linearly filled, including a 15 day hiatus from 16 to 31 July 2007. The boreal summer period was not used in our analysis but will be examined separately in another study. Both SST data sets give qualitatively similar results (see the supporting information), and we use OI data in our composites because of its longer temporal coverage (1981 to present) and smaller biases near land [*Reynolds et al.*, 2007]. This latter point is vital to observations within the MC during convective breaks. Statistical significance was assessed by a Monte Carlo method using 95% confidence levels [*Livezey and Chen*, 1983].

3. Intraseasonal Life Cycles of Convection

[8] Previous studies proposed that IS convectively active phases are, at least in part, a consequence of atmospheric

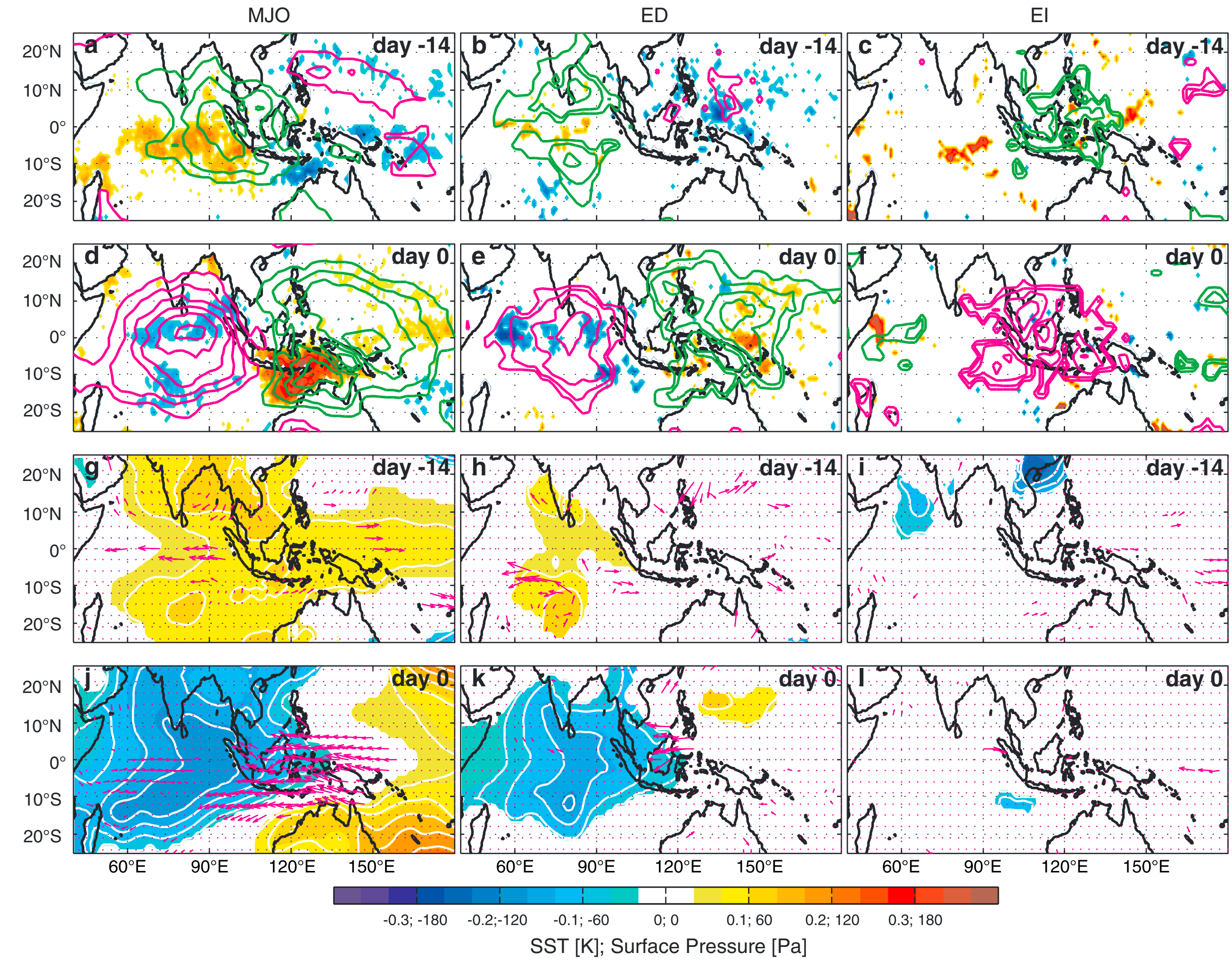

Figure 2. Composites for MJO, ED, and EI events. (a–f) Shading represents significant SST anomalies, and green (magenta) contours represent significant positive (negative) OLR anomalies (5 W m^{-2} intervals). (g–l) Shading represents significant surface pressure anomalies, and vectors represent significant 850 hPa wind anomalies (maximum anomalies of -4.5 m s^{-1} in Figure 2j).

destabilization during the preceding quiescent conditions [*Stephens et al*., 2004; *Agudelo et al*., 2006]. The dynamical mechanism that allows this destabilization period would be an atmospheric Rossby wave response to convective activity to the east, promoting subsidence to the west of convection, sea surface warming, and atmospheric energy buildup [*Wang et al*., 2005]. Sea surface warming is observed during the earlier half of the MJO life cycle (Figure 1c). Overall, OLR leads SST anomalies by around a week. Two weeks prior to maximum MJO convection over the eastern Indian Ocean, easterly anomalies become significant over an anomalously warm equatorial Indian Ocean, while significant cold anomalies prevail under westerlies in the tropical West Pacific (Figures 2a and 2g). The wind and surface pressure anomalies suggest low-level divergent conditions associated with Rossby wave subsidence. The eastward propagation of a Kelvin wave from this region of enhanced subsidence (Figure 2g) suppresses convection along the way and allows warm SST anomalies to grow within the MC. This Rossby-Kelvin wave pair is similar to the large-scale tropical atmospheric response to heating but with the opposite sign. One week before composite day 0 (Figure 1c), convective anomalies grow east of 60°E, while strong positive OLR anomalies sit over the MC and the West Pacific Ocean. On composite day 0 (Figures 2d and 2j), warm SST anomalies are observed south of the equator from Sumatra to New Guinea, under significant low-level easterly anomalies flowing toward the low-level convergence maximum as part of the large-scale wave response to convective heating. These easterly anomalies observed in a region of climatological westerly wind stress indicate decreased evaporative cooling, allowing shortwave flux to raise SST anomalies to the east of active convection [*Woolnough et al*., 2000; *Vialard et al*., 2012]. Convection weakens over the MC, but anomalies near -15 W m^{-2} continue to travel eastward, favored by the positive SST anomalies east of 100°E: these anomalies having developed during the convective break and the wave-related subsidence. The amplitude of easterly anomalies diminishes after the convective peak on composite day 0, suggesting an increase in latent heat flux over the region of anomalously warm SST. The combination of positive IS SST anomalies and a tendency to more westerly wind stress incrementally increases surface heat fluxes to the atmosphere, fuelling further eastward motion. As in the depiction

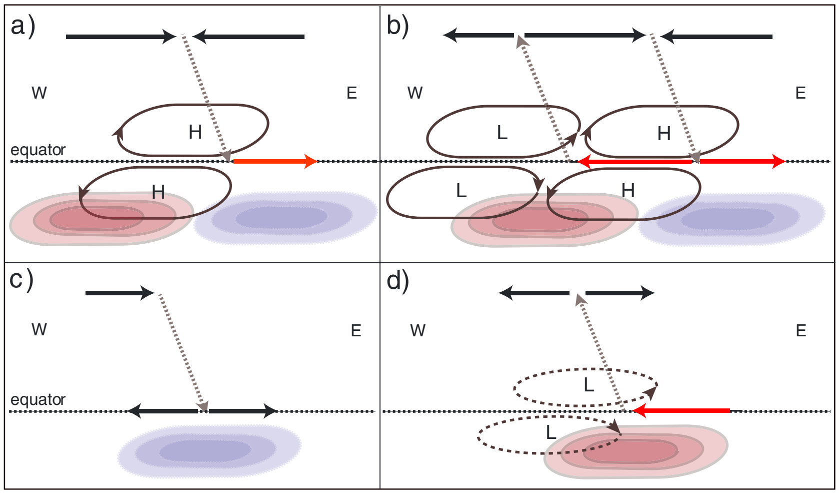

Figure 3. Schematic diagram. (a) Convective break before the MJO. (b) Convective phase for the MJO. (c) Convective break before EI events. (d) Convective phase during EI events. Horizontal dashed lines represent the equator at 850 hPa, above SST positive (red)/negative (blue) anomalies. Dashed arrows represent upward/downward motions between 850 and 200 hPa. Black arrows represent the direction of wind anomalies. Red arrows along the equator indicate 850 hPa winds associated with Kelvin waves. L (H) indicates low-level negative (positive) pressure anomalies.

of the boreal summer IS events by *Wang et al.* [2006], sea surface warming is followed by surface convergence and, subsequently, convection. Propagation is less pronounced for ED and EI events (Figures 1e and 1f). In addition, neither of these IS categories exhibits comparable sea surface warming, leading to convection within the MC.

[9] The convective phases of ED events begin around 1 week prior to maximum convection, as in the MJO cycle (Figure 1e). Weak and incoherent SST anomalies over the initiation region are observed after an earlier break in convective activity (Figure 2b). The convective break moves to the east following the tendency of suppressed convection promoted by the eastward propagation of a dry Kelvin wave. The dynamical signature of the large-scale waves can be identified, but the anomalies are smaller in amplitude and less significant compared to the MJO cycle (Figure 2h). Hence, warm SST anomalies within the MC are also weaker and less significant. It appears that ED events are somehow triggered before the atmosphere-ocean system is able to generate sufficiently strong positive SST anomalies around the MC that sustain further eastward propagation. The weaker influence of large-scale wave dynamics renders the cycle less effective to promote optimal conditions for the growth of SST anomalies to the east and damps the propagation of the convective envelope. Two scenarios could explain the debilitation of eastward propagation: (1) The Rossby wave does not last long enough, and the combination of radiative warming and suppressed evaporative cooling is not able to raise SSTs within the MC; or (2) easterly anomalies associated with the Rossby wave during the convective break are not sufficiently intense to suppress evaporative cooling (Figure 2h).

[10] In the case of EI events, the Rossby and Kelvin waves are completely absent from the composite life cycle (Figures 2i and 2l). There are only small amplitude convective anomalies over the tropical Indian Ocean from day −20 to day −15 (Figure 1f). During the IS break, the region of stronger positive OLR anomalies is centered at 120°E (Figure 2c, day −14), with weak negative anomalies near 60°E and east of 150°E. There is a small tendency of SST warming (although it is not spatially coherent), but positive pressure anomalies observed during the break of convection rapidly decline, and negative anomalies predominate mostly off the equator (Figure 2i). Significant IS perturbations of the zonal circulation over the western Indian Ocean suppress convection to the east 2 weeks before the EI convective maximum, leading to sea surface warming and consequent atmospheric destabilization (Figure S4 in the supporting information). As convection crumbles in the west, negative OLR anomalies grow over the warm pool, east of the MJO initiation region (Figure 2f). One week prior to the convective maximum, negative OLR anomalies begin to deepen over warm SST. A Rossby-Kelvin wave pair only arises after convection develops over the MC. Farther eastward, propagation seems to be solely due to Kelvin waves propagating out of the region. A new convective break seems to develop over the initiation region, while the active IS phase fades away with almost no significant surface circulation anomalies (Figure 2f).

4. Conclusion

[11] The evolution of large-scale tropical IS convection into an MJO event depends on the strength of the interaction between large-scale wave dynamics and radiative processes that begins during a convective break, in agreement with the processes leading to a primary MJO [*Straub*, 2013]. The cycles of an MJO and an ED event begin over the Indian Ocean initiation region, where subsidence generates positive OLR anomalies and surface anticyclones straddling the equator as Rossby waves (Figure 3a). A dry Kelvin wave propagates eastward away from this region, damping convection to the east. These conditions allow sea surface warming by a combination of lower evaporative cooling and radiative heating due to minimum cloud cover. With warm SST anomalies, convection is initiated, generating a Rossby-Kelvin wave response to heating to the west of the convective break (Figure 3b). After the convective phase is active, the entire system propagates to the east. In the MJO cycle, the subsiding Rossby wave that precedes the convective phase is stronger and lasts longer, resulting in

warmer SST anomalies within the MC. These warmer SST anomalies combine with the Kelvin wave propagation to favor the eastward propagation of the entire system across the MC. This subsiding wave is weaker in ED events, resulting in lower or absent positive SST anomalies over the MC and lack of eastward propagation. Previous studies proposed self-regulation [*Stephens et al*., 2004] or self-induction [*Wang et al*., 2005] mechanisms for the maintenance of these convective cycles in which opposite phases would act in a cooperative manner to sustain the oscillation. Our results show that convective breaks are essential for the development of active phases. However, it is not clear that the break phase bears any relationship with a previous IS event as it is suggested by the term *primary MJO* [*Matthews*, 2008]. The amplitude of peak convective anomalies is slightly different for each category and is located over different regions, but the amplitude of positive OLR anomalies generated to the west as convection moves to the east is nearly the same (Figures 1d–1f). Moreover, IS convection generally decorrelates after around one cycle, as indicated by *Hendon and Salby* [1994]. Therefore, the intensity of IS convection is not a good predictor of the subsequent break phase, but the break phase seems to be a good indicator of the following active phase, independent of any autocorrelation or circumnavigation signals.

[12] One may speculate that the life cycle of an IS event is tied to initiation mechanisms in the sense that different triggers could induce distinct convective patterns. Our categorization identifies the event analyzed by *Hsu et al*. [1990], influenced by extratropical disturbances, as an MJO. Extratropical systems play important roles in triggering or organizing IS activity through the tropics [see *Ray and Zhang*, 2010, and references therein]. Nonetheless, the evolution of convection into an MJO event seems to rely more on the mutual interactions of the tropical atmosphere-ocean system immediately before large-scale convective development than on the convective trigger. ED events are somehow triggered before the large-scale wave is able to produce sufficiently large SST anomalies within the MC and debilitates eastward propagation. The triggering mechanism may assume a variety of forms, but the event development and propagation depends on the ability of an IS break to generate SST anomalies to the east of convection. Energy is stored in the ocean during the preceding convective break to be consumed by the subsequent convective disturbance as it progresses to the east. It would be worthwhile to use an independent satellite-determined surface flux data set (e.g., SEAFLUX) [*Curry et al*., 2004]) to confirm the sequence of ocean-atmosphere interactions proposed here. The initiation of EI events occurs independently of equatorial Rossby wave subsidence over the tropical Indian Ocean. Without the Rossby wave influence, no SST anomalies are generated over the usual initiation region, and the convective phase is restricted to a narrower longitude range, exactly where IS convection experiences a minimum in the MJO cycle. The mechanisms behind EI event initiation are not clear as yet and deserve further investigation.

[13] **Acknowledgments.** This work was supported by NOAA grant NA10OAR431016 to the Georgia Institute of Technology. F. E. Hirata was also supported by CAPES/Fulbright grant BEX1842-07/2.

[14] The Editor thanks two anonymous reviewers for their assistance in evaluating this paper.

References

Agudelo, P. A., J. A. Curry, C. D. Hoyos, and P. J. Webster (2006), Transition between suppressed and active phases of intraseasonal oscillations in the Indo-Pacific warm pool, *J. Clim.*, *19*, 5519–5530.

Curry, J. A., et al. (2004), SEAFLUX, *Bull. Am. Meteorol. Soc.*, *85*(3), 409–424.

Hendon, H. H., and M. L. Salby (1994), The life cycle of the Madden-Julian oscillation, *J. Atmos. Sci.*, *51*, 2207–2219.

Hsu, H.-H., B. J. Hoskins, and F.-F. Jin (1990), The 1985/86 intraseasonal oscillation and the role of the extratropics, *J. Atmos. Sci.*, *47*, 823–839.

Kessler, W. S. (2001), EOF representation of the Madden-Julian oscillation and its connection to ENSO, *J. Clim.*, *14*, 3055–3061.

Liebmann, B., and C. A. Smith (1996), Description of a complete (interpolated) outgoing longwave radiation dataset, *Bull. Am. Meteorol. Soc.*, *77*, 1275–1277.

Livezey, R. E., and W. Y. Chen (1983), Statistical field significance and its determination by Monte Carlo techniques, *Mon. Weather Rev.*, *111*, 46–59.

Madden, R. A., and P. R. Julian (1971), Detection of a 40–50 day oscillation in the zonal wind in the tropical Pacific, *J. Atmos. Sci.*, *28*, 702–708.

Matthews, A. J. (2008), Primary and successive events in the Madden-Julian oscillation, *Q. J. R. Meteorol. Soc.*, *134*, 439–453.

Ray, P., and C. Zhang (2010), A case study of the mechanics of extratropical influence on the initiation of the Madden-Julian Oscillation, *J. Atmos. Sci.*, *67*, 515–528, doi:10.1175/2009JAS3059.1.

Reynolds, R. W., T. M. Smith, C. Liu, D. B. Chelton, K. S. Casey, and M. G. Schlax (2007), Daily high-resolution blended analyses for sea surface temperature, *J. Clim.*, *20*, 5473–5496.

Stephens, G. L., P. J. Webster, R. H. Johnson, R. Engelen, and T. L'Ecuyer (2004), Observational evidence for the mutual regulation of the tropical hydrological cycle and tropical sea surface temperatures, *J. Clim.*, *17*, 2213–2224.

Straub, K. (2013), MJO initiation in the real-time multivariate MJO index, *J. Clim.*, *26*, 1130–1151.

Vialard, J., K. Drushka, H. Bellenger, M. Lengaigne, S. Pouls, and J. P. Duvel (2012), Understanding Madden-Julian-induced sea surface temperature variations in the North Western Australian basin, *Clim. Dyn.*, doi:10.1007/s00382-012-1541-7, in press.

Wang, B., P. J. Webster, and H. Teng (2005), Antecedents and self-induction of active-break South Asian monsoon unraveled by satellites, *Geophys. Res. Lett.*, *32*, L04704, doi:10.1029/2004GL020996.

Wang, B., P. J. Webster, K. Kikuchi, T. Yasunari, and Y. Qi (2006), Boreal summer quasi-monthly oscillation in the global tropics, *Clim. Dyn.*, *27*, 661–675.

Wentz, F. J. (1997), A well-calibrated ocean algorithm for Special Sensor Microwave/Imager, *J. Geophys. Res.*, *102*, 8703–8718.

Wheeler, M. C., and H. H. Hendon (2004), An all-season real-time multivariate MJO index: Development of an index for monitoring and prediction, *Mon. Weather Rev.*, *132*(8), 1917–1932.

Woolnough, S. J., J. M. Slingo, and B. J. Hoskins (2000), The relationship between convection and sea surface temperature on intraseasonal timescales, *J. Clim.*, *13*, 2086–2104.

Zhang, C. (2005), Madden-Julian oscillation, *Rev. Geophys.*, *43*, RG2003, doi:10.1029/2004RG000158.